Science of the Total Environment 909 (2024) 168413

Contents lists available at ScienceDirect

Science of the Total Environment

journal homepage: www.elsevier.com/locate/scitotenv

Dispersion and stratification of *Per*-and polyfluoroalkyl substances (PFAS) in surface and deep-water profiles: A case study of the Biscayne Bay area

Olutobi Daniel Ogunbiyi, Neumiah Massenat, Natalia Quinete *

Department of Chemistry and Biochemistry, Florida International University, 11200 SW 8th St, Modesto Maidique Campus, Miami, FL, 33199, USA
Institute of Environment, Florida International University, 11200 SW 8th St, Modesto Maidique Campus, Miami, FL, 33199, USA

HIGHLIGHTS

- Vertical PFAS profile shows surface-enrichment, depth-depletion pattern.
- PFOS/PFOA >1 suggests that point sources are the major contribution to PFAS burden.
- IDW model predicted the contribution of oceanic current on the dispersion of ∑PFAS.
- K-Means clustering shows location with common PFAS fingerprints.
- LDI suggests source contribution of PFAS contamination in the Biscayne Bay.

GRAPHICAL ABSTRACT

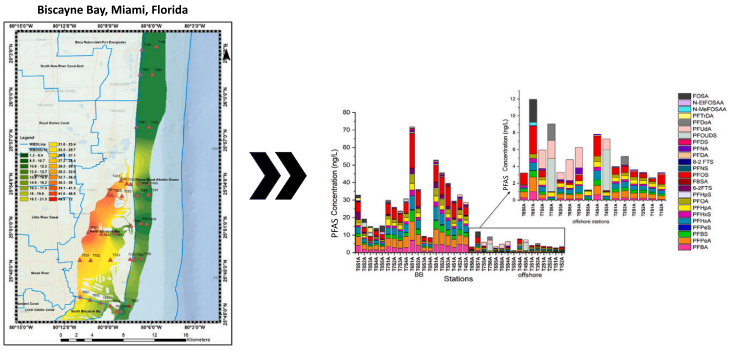

ARTICLE INFO

Editor: Damiá Barceló

Keywords:
PFAS loading
Vertical profile
Costal environment
LC-MS/MS
Miami-Dade
South Florida

ABSTRACT

Per-and polyfluoroalkyl substances (PFAS) are a group of synthetic chemical compounds known for their persistent, bioaccumulation and toxic characteristics in all environmental compartments. As industrial and domestic applications of PFAS increase, their discharge into water bodies becomes of human and ecological concerns. Our research focuses on providing better understanding on the occurrence, vertical distribution, and dispersion of PFAS in surface and bottom water from inshore and offshore area of Biscayne Bay, Miami, Florida. We screened a total of 30 PFAS from inshore (N = 38) and offshore (N = 48) water samples using a semi-automated solid phase extraction (SPE) followed by instrumental analysis using Liquid chromatography-mass spectrometry techniques (LC-MS/MS). Our findings show a general surface-enrichment and depth-depletion pattern from inshore to offshore area. Average ∑PFAS loadings inshore (surface vs bottom; 29.52 ± 15.26 ng/L vs 21.45 ± 7.85 ng/L) is significantly greater than offshore (surface vs bottom; 5.18 ± 2.68 ng/L vs 2.42 ± 2.11 ng/L). PFOS had the highest mean concentration both inshore (6.36 ± 4.23 ng/L) and offshore (0.83 ± 0.87 ng/L). The most frequently detected (D·F > 91 %) PFAS are Perfluorooctane sulfonic acid (PFOS), Perfluorooctanoic acid (PFOA), Perfluoroheptanoic acid (PFHpA), Perfluorohexanoic acid (PFHxA), Perfluorobutanoic acid (PFBA), Perfluorobutane sulfonic acid (PFBS) and Perfluorohexane sulfonic acid (PFHxS) in surface water samples. PFOS/PFOA >1 suggests that point sources are the major contribution to PFAS burden in the Biscayne Bay. An innovative Inverse distance weighted interpolation (IDW) special modelling approach was implemented to predict the potential contribution of oceanic current on the dispersion of ∑PFAS loadings in

* Corresponding author.
E-mail address: nsoaresq@fiu.edu (N. Quinete).

https://doi.org/10.1016/j.scitotenv.2023.168413
Received 1 September 2023; Received in revised form 5 November 2023; Accepted 5 November 2023
Available online 8 November 2023

surface and bottom profiles from canals (inshore) to offshore areas. This will provide insights into transport mechanisms of PFAS from source emissions, and risk assessments of potential impacts on human and aquatic life in the Bay.

1. Introduction

Per-and polyfluoroalkyl substances (PFAS) are a group of anthropogenic contaminants that are deleterious to human and aquatic health. For >50 years, PFAS have been used in personal care products, water-repellent coatings, adhesives, and aqueous fire-fighting foams (AFFF) (Susmann et al., 2019; Zhao et al., 2012). The chemistry of these compounds characterized by strong C—F bond and thermal stability makes them persistent and ubiquitous in all environmental compartments. They have been detected in water, air, sediments, fish, and humans because of long-term manufacture and numerous applications (Chiumiento et al., 2023; Herzke et al., 2023; Li et al., 2022; Ogunbiyi et al., 2023; Scher et al., 2018). This calls for human and ecological concern as they are precursors to immunological disorders, endocrine, developmental, reproductive, and neurological disruption (Chang et al., 2016; Louisse et al., 2020). Additionally, PFAS can also be released into the environment through point sources such as wastewater treatment plants (WWTPs), domestic and industrial facilities and landfill leachates while non-point sources are released through precipitation, surface runoffs from industrial, agriculture and wastewater worldwide. Furthermore, atmospheric transport and degradation of volatile precursors are alternative source of PFAS in the ocean (Han et al., 2022). Hence it is important to understand the occurrence and distribution of these contaminants in coastal environments, which can represent a threat to a variety of marine organisms.

As reported in previous studies, significant amount of PFAS were detected in Biscayne Bay and adjacent canals in South Florida (Li et al., 2022). South Florida is characterized by a unique and flourishing ecosystem that ultimately combines various elements such as urban and rural areas, swamps, marshes (e.g., the Florida Everglades) and bays (Mcpherson et al., 1976). Biscayne Bay is a prominent and monumental feature in South Floridan ecosystems. It is described as a sub-tropical estuary situated between the mainland and barrier islands, adjacent to the city of Miami. The Biscayne Bay ecosystem is of tremendous ecological importance, and it supports a wide variety of invertebrates, fishes, American crocodiles, dolphins, and manatees. However, Biscayne Bay, especially the Northern section suffers from habitat loss, excessive nutrient loads, reduce water transparency and sewage discharge contamination due to heavy urbanization and industrial activities (Caccia and Boyer, 2005). This can potentially lead to increased environmental contamination by organic chemicals such as PFAS commonly present in wastewater and septic effluents, consequently endangering the flourishing coral and marine community in Biscayne Bay. Other findings suggest that the canals are major point sources of discharge of contaminants into the Bay (Caccia and Boyer, 2007; Lirman et al., 2008; Ng et al., 2022). Li et al. in 2022 reported high PFAS loadings in adjacent canals located in the northern section of the Bay (Li et al., 2022).

With the massive influx of freshwater into the Bay, it is crucial to understand the occurrence and dispersion of PFAS from the point of discharge (canals) through intercoastal settlements into the Atlantic Ocean as well as investigate potential contribution of environmental factors such as ocean current, temperature, and salinity on their stratification in the water column. Hence, the aim of this research is to provide further insights on the surface distribution of PFAS from West of the canals to East- coastal areas of the Biscayne Bay. We have also studied the vertical migration of PFAS from surface to deep waters both inshore and offshore to confirm the major point source of intrusion of these contaminants into the Bay. In addition, this research also seeks to explain the influence of ocean currents, salinity, and temperature in the distribution of PFAS from inshore to coastal environment of Biscayne Bay.

2. Materials and methods

2.1. Sample collection

Water samples were collected between 9th June to 14th of June 2022 at Biscayne Bay, located in Miami-Dade County, Florida. Brackish water samples from inshore, Biscayne Bay ($N = 38$) and sea water samples ($N = 48$) were taken offshore as shown in Fig. 1 using a previously cleaned Niskin bottle (Oceanics. Inc., Miami, FL) for sample collection. The Niskin bottle was cleaned using Liquinox soap and rinsed with ultrapure water before each sampling event. The stations where the samples were collected are also indicated in Fig. 1 and geographical coordinates are available in Table S1 and S2. Each station was sampled once in 3 different sampling events (June 9th, 13th and 14th, 2022) by boat, encompassing representative areas of the Bay with influence from freshwater canals into the Northern section of Biscayne Bay, whereas wind speed ranged from 1.3 to 3.4 m/s in June 9th, 2.8–4.1 m/s in June 13th and 3.0–4.0 m/s in June 14th, and wind direction from 44 to 180 degT, 75–88 degT and 69–88 degT, respectively (NOAA, 2023), showing similar conditions on the different sampling days. The inshore water samples were taken in the surface at a depth of 0–0.5 m and bottom (~4 m depth) while offshore sea water samples were taken at surface (0-1 m), subsurface (~5 m) and bottom (~8–10 m) as shown in Fig. 2. Longitudinal transects (80.2 ^{0}N to 80.1 ^{0}W) were conducted from the Biscayne Bay inshore areas to offshore. Biscayne Bay (25 ^{0}N-26 ^{0}N and 80 ^{0}W-85 ^{0}W), a typically shallow estuarine lagoon extending almost the length of Miami-Dade County, is in the southeastern part of Florida. It is notable for its unique mangrove plants, flourishing coral reef ecosystem and habitat to diverse recreational fisheries. An Exode2 sonde (Ysi.Inc. /xylem.Inc., OH., USA) with seven probes was used for in-situ measurements of environmental parameters such as temperature, salinity, chlorophyll level, pH, turbidity, and conductivity. Sample bottles (0.5 L Polypropylene) were rinsed in the lab with Methylene chloride, hexane, acetone, and methanol (twice) to remove any potential PFAS background contamination before sampling events. The samples were transported in ice into the laboratory and stored at 4 °C in the refrigerator until analysis.

2.2. Chemicals and reagents

Extracting and mobile phase solvents- Methanol, ammonium hydroxide, LC-MS grade water and cleaning solvents- acetone, hexane, methylene chloride were obtained from Fisher scientific (Waltham, USA). A total of 30 PFAS were analyzed. PFAC30PAR (1 μg/mL in MeOH) consisting of 30 PFAS native standard solutions including perfluorocarboxylic acids (PFCAs) (C4-C14), perfluorosulfonic acids (PFSAs) (C4-C10 linear chain; C6 and C8 branched chain isomers), where PFOS (linear + branched chain), perfluorooctanesulfonamide PFOSA (C4, C6, and C8), linear and branched isomers of *N*-methyl perfluorooctanesulfonamidoacetic acid (N-MeFOSAA) and N-Ethyl perfluorooctanesulfonamidoacetic acid N-EtFOSAA, Gen X (HFPO-DA), and fluorotelomer alcohols (4:2 FTS, 6:2 FTS and 8:2 FTS) were purchased from Wellington laboratories (Guelph, Canada). The isotopically mass labeled standards MPFAC-24ES (1 μg/mL in MeOH) and M3HFPO-DA (50 μg/mL in MeOH) were also purchased from Wellington laboratories. Working solutions of PFAS native standards (1 ppb and 10 ppb) were prepared from PFAC30PAR in LC-MS grade water while a secondary standard (PFC-24, 2 μg/mL in MeOH) purchased from

AccuStandard (New Haven, USA) was used as the initial calibration verification (ICV). All the Strata weak anionic exchange (WAX) cartridges (500 mg, 3 mL) used for the Solid Phase Extraction (SPE) were obtained from Phenomenex Inc. (Torrance, CA). The list of PFAS present in the native standard, ICV and isotopically labeled mixtures are shown in Table S3.

2.3. Extraction methodology and instrumental analysis

Water samples collected from our study location were not filtered to prevent potential loss of PFAS caused by sorption to the filter paper (Han et al., 2022; Joerss et al., 2020). A previously developed and validated semi-automated offline SPE technique was used for the extraction and preconcentration steps of PFAS from the water samples (Li et al., 2022). In succinct, 250 mL of the water samples were spiked with 100 μL of an isotopically labeled internal standard (IS) mixture at a concentration of 2.5 ng/L followed by extraction step using SPE. An SPE cartridge (Strata-XL-AW, Phenomenex Inc., Torrance, CA) composed of a hydrophobic-diamino complex was utilized for the extraction of PFAS. The cartridges were preconditioned with 6 mL of NH_4OH: MeOH (0.3: 99.7 %) and methanol followed by equilibrating with LC-MS grade water. The samples were loaded into the cartridge at 10 mL/min while the sample bottles were rinsed (twice) with 5 mL of LC-MS water to ensure complete introduction of the samples into the cartridge. The cartridge was left for 40 min under vacuum to dry and then eluted with 10 mL of NH_4OH: MeOH (0.3: 99.7 %) into a sample vial for evaporation to dryness under a gentle stream of nitrogen evaporator operated at 40 °C to prevent the loss of volatile long chained PFAS.

The extract was reconstituted using 1 mL of ammonium formate in methanol (*v*/v; 90: 10 %) and transferred into a polypropylene LC-MS autosampler vial for instrumental analysis. A liquid chromatographic system (Agilent 1290 Infinity II) hyphenated to an QqQ mass spectrometry (Agilent 6470) was operated in negative electrospray ionization (LC-(−)ESI-MS/MS) for the detection and quantification of PFAS. An analytical column Hypersil GOLD pentafluorophenyl column (150 mm × 2.1 mm, 3 μm) maintained at 50 °C and a mobile phase consisting of 5 mM ammonium formate buffer and methanol gradient was used for the PFAS separation. A delay column (Hypersil GOLD aQ C18, 20 × 2.1 mm, 12 μm) was installed before the injection system. Detailed info on MS and chromatography conditions including MRM transitions are reported elsewhere and shown in the supplementary info Tables S4 to S6 (Li et al., 2022).

2.4. Quality assurance and quality control measures

To prevent any cross-contamination, all the LC-MS/MS and SPE tubbing's were replaced with PFAS-free plastics. Fields blanks (composed of 0.5 L of LC-MS grade H_2O) which primarily served as the negative control was poured into the Niskin bottle prior sampling to screen for background contamination from the water sampler. Although the concentration of field blanks was marginally higher than the laboratory blanks, the results obtained from this experiment were corrected by subtracting the concentration of each PFAS in the field blank from the environmental samples. In order to ensure the quality and accuracy of our experimental data, negative controls (field blanks and method blanks), positive control (prepared by spiking 250 mL of LC-MS grade H_2O with 10 μL of 10 ppb of native standard and 100 μL of internal standard), as well as a continuing calibration verification standard

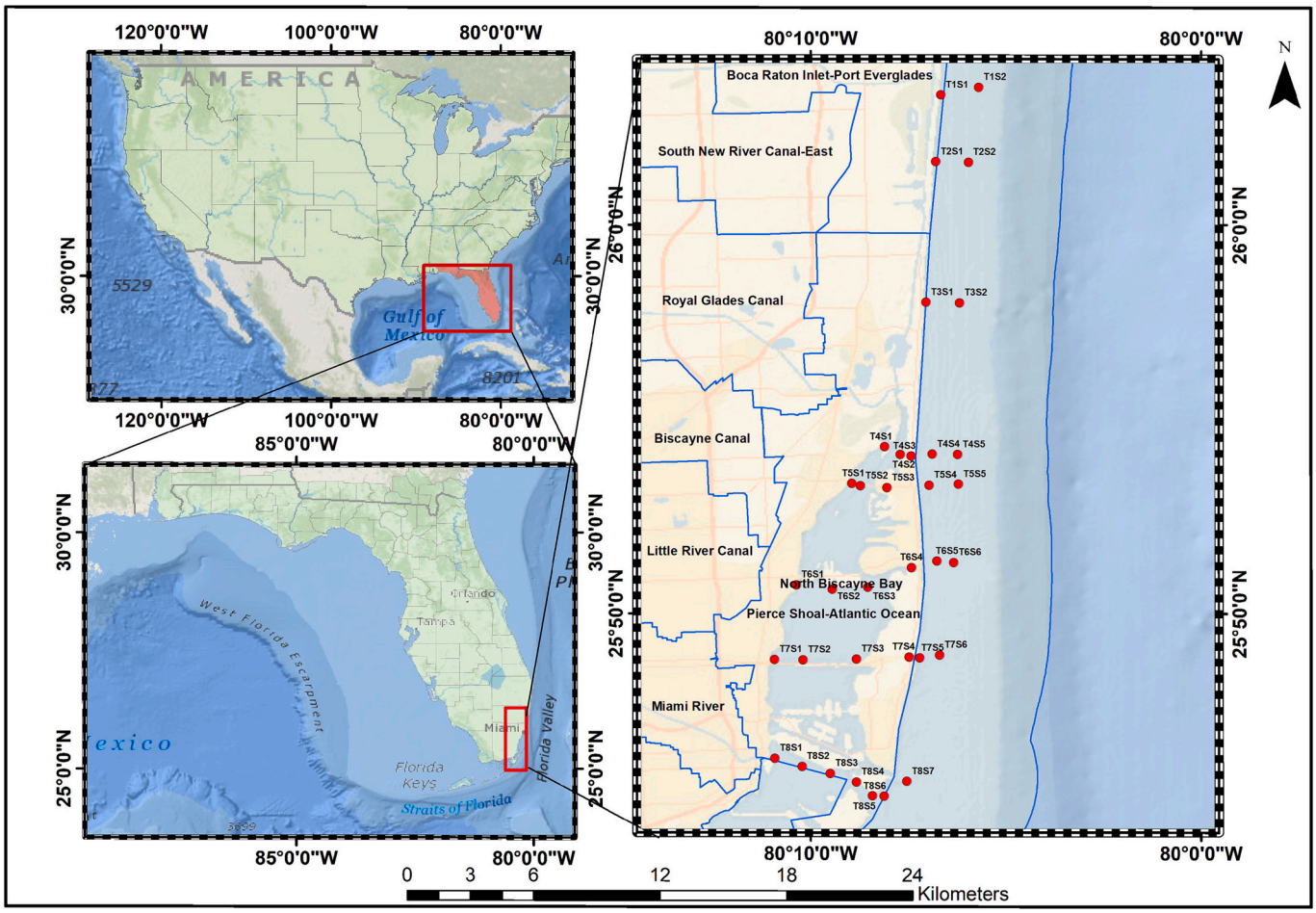

Fig. 1. Map showing the Longitudinal transects of sampling stations in the Biscayne Bay (Miami-Dade County, Florida) coastal and offshore areas.

(CCV) at a concentration of 100 ng/L and ICV's were added after every 10 samples and included in each batch. An 11-point calibration curve was run at the beginning and end of the sequence to confirm linearity. Concentration of PFAS ranging from 2 to 1000 ppt were prepared in LC-MS grade water for the calibration curve and linearity was achieved by estimating the coefficient of variance ($R^2 > 0.99$) using the Agilent MassHunter QQQ Quantitation analysis software (Table S7). However, it was observed that $R^2 < 0.99$ for some specific long-chained PFAS such as: PFTrDA, PFTeDA, PFDoA, PFOUDS and PFDS (ranging from 0.97 to 0.98) as also reported by (Li et al., 2022). Instrument detection limits (IDLs) and method detection limits (MDLs) for each PFAS have been established in a previous study published elsewhere (Li et al., 2022). MDL ranged from 0.01 (PFBS) -1.99 ng/L (PFTeDA) while IDL ranged from 0.26 (PFBA) to 205 ng/L (PFTeDA) as shown in Table S7. To determine the precision of our results, duplicate samples were collected and analyzed for PFAS. The variability of the measured concentration of PFAS was $< \pm 14.5$ % (mean $\pm$ SD; 20.85 $\pm$ 2.97 ng/L). Matrix and blank spiked samples were also analyzed to determine potential interference emanating from high salt content which can cause ion suppression or enhancement of analyte signals. Average recoveries (%) were calculated to determine the potential loss of analyte during sample preparation processes (Table S7). Results obtained by comparing spiked samples with unspiked samples showed the range of 68–125 % for most PFAS except for PFDS (38 %), PFNS (44 %), FHxSA (50 %) and PFOUDS (153 %).

2.5. Data processing and statistical analysis

Analyzed datasets were processed using Agilent MassHunter QQQ Quantitative analysis software (Quant-my-way, version 10.0). Peak peaking and integration of PFAS analytes were programmed to similar retention time to the labeled standard ($\pm$0.1 min) and S/N > 3. Analytes without labeled standards were quantified using labeled standards with similar chemical structures (functional group and chain length). All statistical analysis for the dataset was done using R software (version 4.1.1: (C) 2021). For statistical purposes, concentrations <MDL were treated as ½ MDL for each PFAS. The normality of the dataset was tested using Shapiro-Wilks test ($p > 0.05$). The results obtained indicates non-normality, hence, non-parametric test such as Mann-Whitney-Wilcoxon test was applied to assess the statistical significance between two independent groups inferred at $p < 0.05$ e.g., $\sum$ PFAS inshore and offshore of Biscayne Bay. Also, other variables such as depth and concentration of PFAS inshore were also statistically analyzed. Kruskal-Wallis's test was used to determine the statistical significance between three independent groups ($p < 0.05$). Post-hoc test was used to assess groups that are statistically different from others. Finally, Spearman's rank correlation plot was utilized to examine the relationship between the concentration of PFAS in surface water profiles against salinity.

3. Results and discussion

3.1. Latitudinal transects of legacy and emerging PFAS occurrence and distribution from inshore to offshore areas of the Biscayne Bay

Surface and bottom water samples were collected in transects (Fig. 1), whereas Transect 1–3 which are solely offshore samples (Northward side of the map) and Transect 4–8 each containing different sites were screened for 30 PFAS. The sites span from the canal structures in the Bay (left side of the map) and connect to offshore (boundary with the Atlantic Ocean). PFAS concentrations in surface and bottom surface water are shown in Table S8. Surface profile indicates a general decline (dilution) in PFAS concentrations in all the transects from sites close to

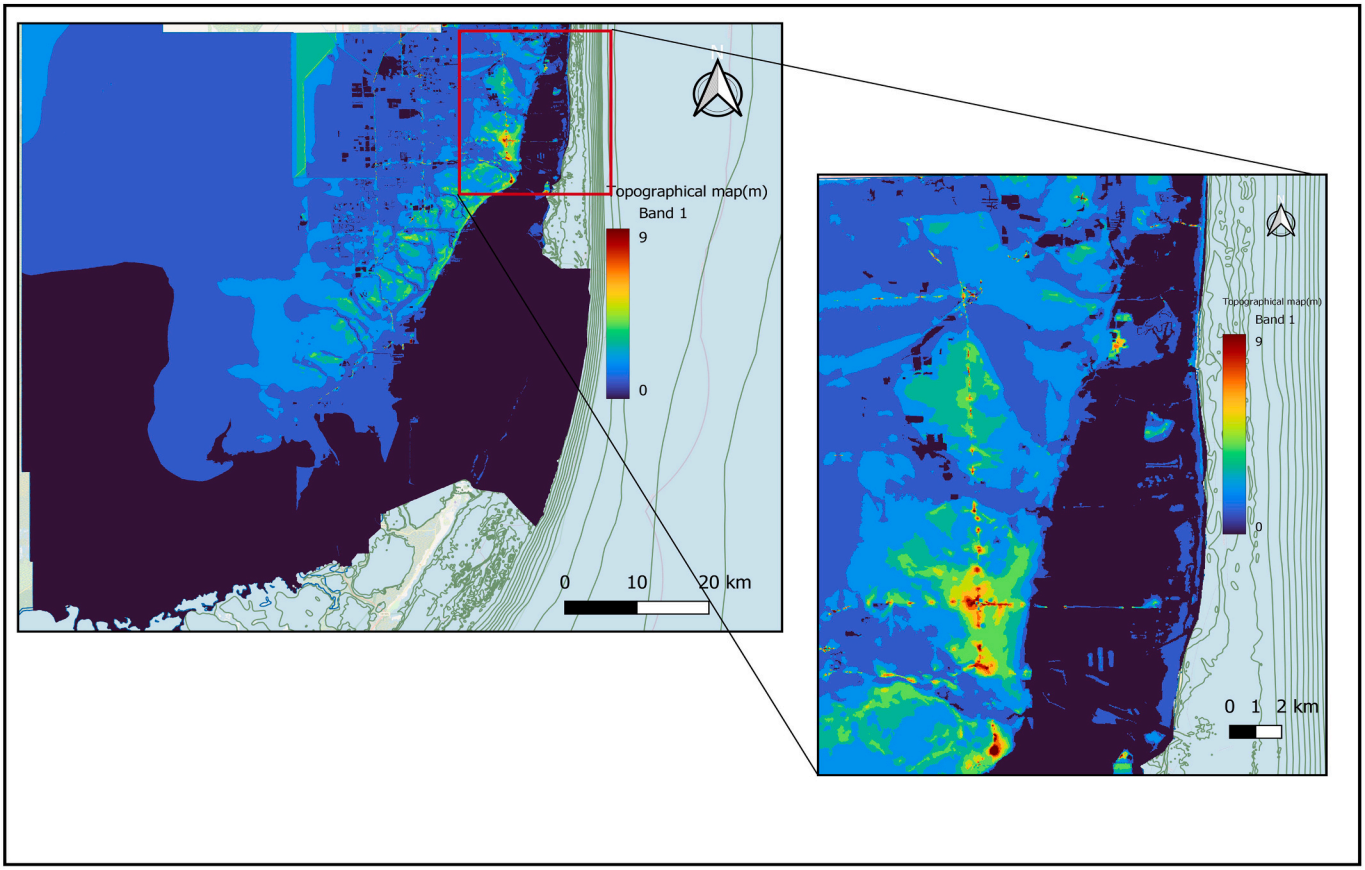

Fig. 2. Topographical and oceanic Bathymetric data showing different depths of the Biscayne Bay coastal areas to the sea level.

the point sources towards offshore areas, except for sites T8S5A (∑PFAS = 15.77 ng/L), T4S2A (∑PFAS = 33.17 ng/L) and T7S4A (∑PFAS = 30.99 ng/L) which were situated close to intercoastal, urbanized areas (Fig. 3). Of all the stations sampled in the Bay, station T6S1A had the highest PFAS concentration (∑PFAS = 72.04 ng/L) followed by station T5S1A (∑PFAS = 53.14 ng/L) situated near the Biscayne canal. These canals (including the Miami river) are characterized as the largest inflow of freshwater into the northern section of the Biscayne Bay. Moreso, stormwaters from urbanized uplands are reported as major contribution of pollutants and nutrient discharge through these canals (Caccia and Boyer, 2007). Detection frequency (D·F) and mean concentration (X ± S·D) were used to describe the most prevalent PFAS in both locations. Average surface PFAS concentration inshore is 29.52 ± 15.25 ng/L while offshore is 5.17 ± 2.66 ng/L. ∑PFAS concentration range from 8.56 ng/L (T6S4A) to 71.80 ng/L (T6S1A) within the Biscayne Bay while offshore concentration ranged from 1.22 ng/L (T5S5A) to 11.96 ng/L (T8S7A) located along the southern valve (Government cut water ways) which receives wastewater from Miami river. Mann-Whitney two-tailed test (α = 0.05) indicates statistical difference ($p < 0.05$) between the ∑PFAS inshore and ∑PFAS offshore. Of all the 30 PFAS screened in our location, Adona, GenX, 4-2FTS, PFONS, FHxSA and PFTeDA were not detected in surface water inshore. The PFOS was the most predominant compound found in all the stations ranging from 2.24 to 19.84 ng/L within the Bay and < MDL to 3.30 ng/L offshore. Other PFAS (average ± S·D) such as PFPeA (4.89 ± 2.33 ng/L), PFBA (3.14 ± 1.55 ng/L), PFHxA (3.82 ± 1.99 ng/L), PFBS (2.32 ± 1.49 ng/L), PFOA (1.97 ± 1.23 ng/L), PFHpA (1.88 ± 1.10 ng/L), PFHxS (1.33 ± 0.78 ng/L), and PFNA (0.45 ± 0.32 ng/L) were frequently detected in inshore samples (D·F ≥94 %). Other PFAS detected in >65 % of the samples were PFHpS (0.16 ± 0.13 ng/L; D·F = 89 %), PFPeS (0.11 ± 0.12 ng/L; D·F = 84 %) and 6-2FTS (1.08 ± 1.17 ng/L; D·F = 68 %). Apart from PFOS (0.83 ± 0.87 ng/L; D·F = 87.5 %) with the highest mean concentration offshore, other PFAS found in offshore surface samples includes PFPeA (0.58 ± 0.42 ng/L; D·F = 81.25 %), PFHxA (0.54 ± 0.25 ng/L; D·F = 100 %), PFHpA (0.42 ± 0.17 ng/L; D·F = 87.5 %), PFBS (0.30 ± 0.18 ng/L; D·F = 100 %), PFBA (0.24 ± 0.24 ng/L; D·F = 81.25 %), PFOA (0.23 ± 0.18 ng/L; D·F = 81.25 %), and PFHxS (0.21 ± 0.10 ng/L; D·F = 100 %). Although, PFOUDS (0.55 ± 1.45 ng/L; D·F = 12.5 %) and PFUdA (0.71 ± 0.99 ng/L; D·F = 37.5 %) had high mean concentration offshore after PFOS, their detection frequency was very low compared to other PFAS reported. In terms of locations sampled offshore, PFHpA (0.65 ng/L), PFHxA (1.09 ng/L), and PFOA (0.63 ng/L) were highest in station T4S4A compared to others. T4S4A is located at the opening of Bal Harbor waterways and close to the outfall pipes that discharge treated effluents from the Miami Dade's North District wastewater treatment plant (WWTP). These compounds are commonly reported in WWTPs effluents due to their poor removal (Lenka et al., 2021; Li et al., 2020; Lorenzo et al., 2019; Rundle et al., 2019). The percentage composition of each PFAS in surface profile is shown in Fig. 4. The results suggest that the % composition of PFAS inshore apparently differs from offshore stations. Unlike offshore sites with different composition of PFAS, inshore sites are similar among each other, suggesting a similar PFAS pollution source. Overall, the % composition of very long chain C9-C14 offshore is higher than inshore stations, which indicates that coastal environments can indeed accumulate legacy PFAS.

3.2. Vertical profile of PFAS and ∑ PFAS from inshore to offshore areas of the Biscayne Bay water column

Fig. S1A-C shows the vertical profile of all 30 PFAS screened in our study area from West (close to the canal shorelines) to East (towards the Atlantic Ocean) and up North at the mouth of the Stranahan river which is south-west to Fort Lauderdale-Hollywood International Airport to the South (close to the Rickenbacker Causeway, Florida). Water samples were collected at surface (0 m) and bottom (~4 m) inshore while surface water samples (0 m), subsurface (~5 m) and bottom (~9–10 m) were collected from offshore since the sea bathymetry parameters differs from inshore to offshore (Fig. 2). Vertical profile of PFAS indicates a "surface-enrichment and depth-depletion" model except for some long chain congeners inshore (PFDoA, PFTrDA and PFUdA) and offshore (PFDA and PFDoA) that showed higher concentrations probably due higher organic carbon-water coefficient (K_{OC}) which facilitates sorption to particulate matter especially for longer chain PFAAs (> C9) (Göckener et al., 2022; Savvidou et al., 2023). Furthermore, it has also been reported that there is an inverse relationship between salinity and PFAS concentration in saline environments (Joerss et al., 2020). This explains differences in concentration observed inshore as the water is characterized by fresh water on the surface and salty water sweeping across the bottom from the Atlantic Ocean. Similarly, the same trend in depth-depletion was observed offshore for PFAS suggesting that the physical pump plays a crucial role in the sinking and vertical

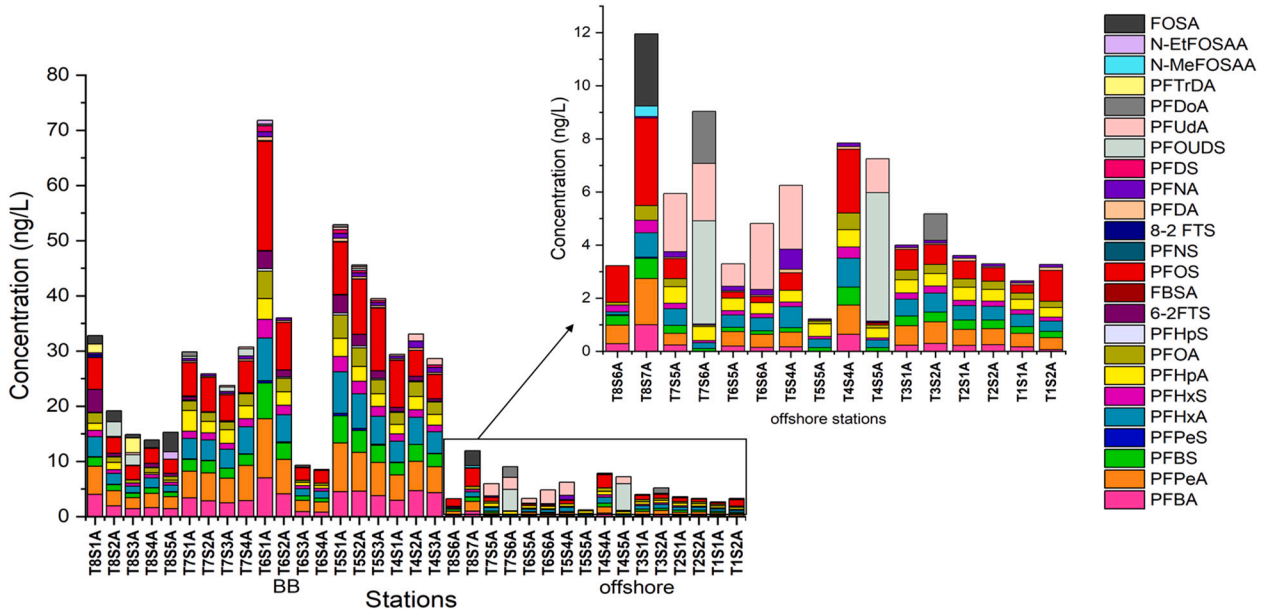

Fig. 3. Component bar chart showing the distribution of PFAS in surface water from inshore to offshore areas of the Biscayne Bay.

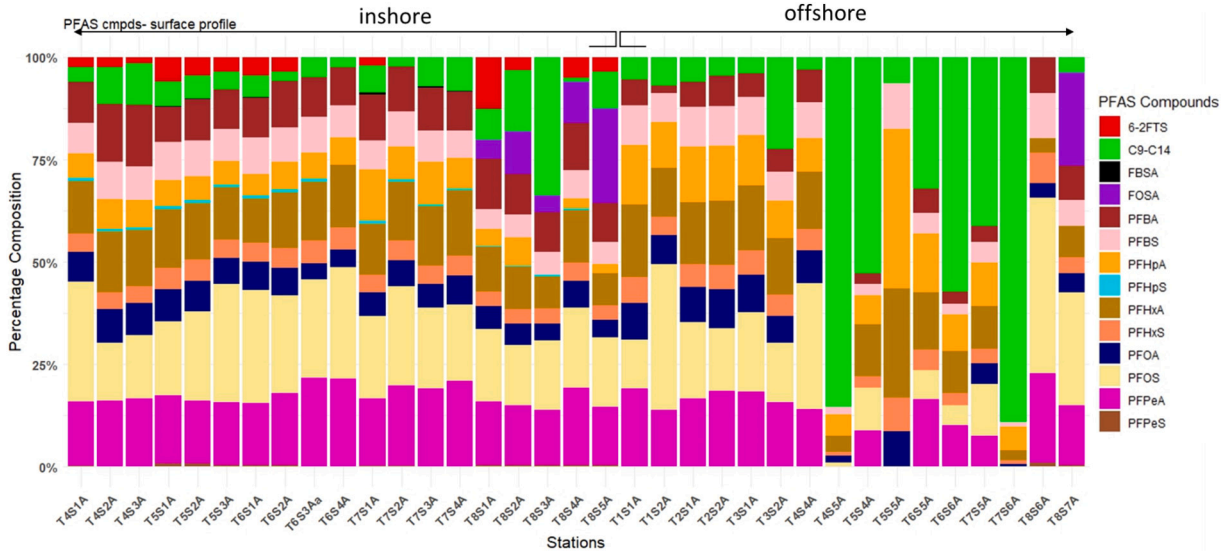

Fig. 4. Percentage composition of PFAS in surface water collected in stations from inshore and offshore Biscayne Bay area, Miami, Florida. Long chain PFAS with C9-C20 were grouped for all the stations sampled.

distribution of PFAS. Unlike other persistent hydrophobic contaminants such as organochlorinated pesticides (OCPs) and polycyclic aromatic hydrocarbons (PAHs) that are reported to be prevalent at the oceanic floor due to high propensity for particle-mediated transport through adsorption with settling biogenic particles (also known as the biological pump), most PFAS (except long chain PFAAs) are relatively stable and deplete gradually with depth by wind action, resuspension and eddy diffusion (Han et al., 2022; Joerss et al., 2020; Lescord et al., 2015; Yamazaki et al., 2019; Zhang et al., 2019)). The % composition of PFAS in surface (Fig. 4) and bottom (Fig. 5) profile from inshore to offshore varies from station to station and highlights the potential contribution of different sources such as freshwater inflow, ocean current and physical pump on their distribution. Wilcoxon rank paired test ($\alpha = 0.05$) shows a statistical significance ($p < 0.05$) between the individual PFAS and $\sum$PFAS burden found in the surface and bottom at inshore and offshore sites respectively except for compounds (ADONA and GenX) that were absent in both surface and bottom profile, inshore.

Fig. 6 shows the vertical profile of $\sum$ PFAS collected from inshore to offshore Biscayne Bay. The $\sum$PFAS inshore from surface to bottom water follows a depth depletion pattern except for T8S5 (Surface vs bottom; 15.30 ng/L vs 22.74, $p = 6.287E\text{-}3$) which was collected at the South-Eastern valve, close to Rickenbacker Causeway. The water in this region is characterized by upwelling and overturning of surface freshwater (from the Miami river) with the incoming tidal-saline water coupled with turbulent wind action which could have aided the rapid transfer of PFAS from surface to bottom. Other stations with similar trend include T7S2 (surface vs bottom; 25.85 ng/L vs 26.63 ng/L, $p = 1$), T7S4 (Surface vs bottom; 30.71 ng/L vs 35.85 ng/L, $p = 0.9265$), T6S3 (surface vs bottom; 9.30 ng/L vs 13.98 ng/L, $p = 6.836E\text{-}3$) and T6S4 (surface vs bottom; 8.56 ng/L vs 20.20 ng/L, $p = 2.441E\text{-}4$). These stations are in intercoastal urbanized settlements. Underground leakage of sewer pipes, septic tanks, and wastewater from water treatment facilities

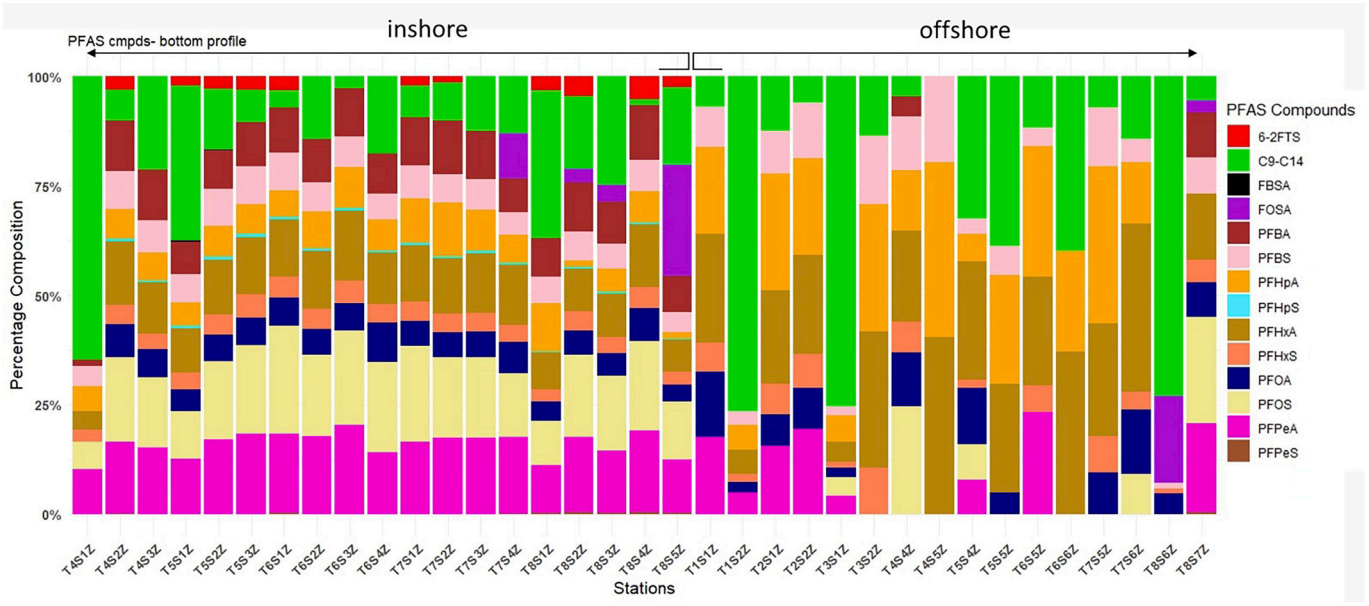

Fig. 5. Percentage composition of PFAS in bottom water collected in stations from inshore and offshore Biscayne Bay area, Miami, Florida. Long chain PFAS comprising of C9-C20 were grouped in all the stations sampled.

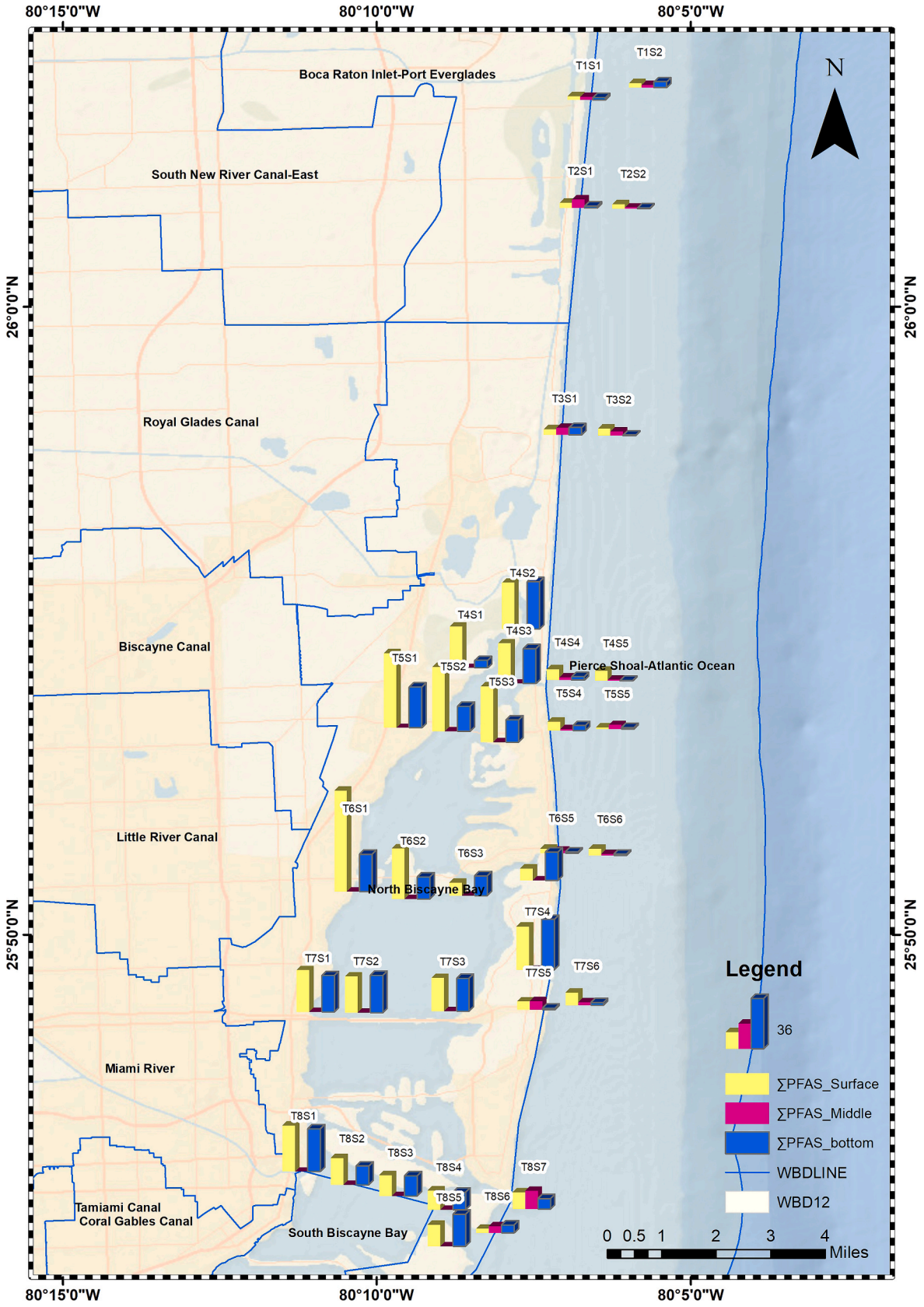

Fig. 6. Vertical profile of ∑PFAS from inshore to offshore. *Subsurface samples were only collected for offshore represented in the graph as ∑PFAS_Middle.*

are believed to be responsible for higher ∑PFAS loadings in bottom waters in addition to particulate resuspension. It is also interesting to note that although T6S1A (Little River transect) had the highest ∑PFAS loadings (71.80 ng/L) compared to T8S1A (32.81 ng/L at Miami River transect), the width of Miami river opening into the Bay (~308 m) is two times that of Little river canal (~144 m). This might explain why PFAS concentrations are more diluted at the Miami River transect due to larger volume of freshwater entering the Bay through this river. Observed ∑PFAS (surface vs bottom) at T8S3 (14.88 ng/L vs 14.38 ng/L, $p = 0.8176$) and T8S4 (13.88 ng/L vs 12.60 ng/L, $p = 0.3757$) suggests fair mixing from surface to bottom due to action of moving turbines from boats and ferries plying through the waterways to and from the Port of Miami. In general, ∑PFAS decreases as we migrate from the canals through the barrier Islands to the Atlantic Ocean (Fig. S2 and S3). The surface ∑PFAS loadings offshore appears to increase from west (coastal shoreline) to east (forward to the Atlantic Ocean) as observed in all the transects (from up-North to down-South) except for Transect 5 (T5S4A vs T5S5A; 6.23 ng/L vs 1.22 ng/L) and Transect 4 (T4S4A vs T4S5A; 7.84 ng/L vs 7.24 ng/L). This fluctuation is attributed to the action of wind and ocean currents (majorly Florida current which blows in the coastal area of Biscayne Bay to up North). Furthermore, station T8S6 (surface vs bottom; 3.23 ng/L vs 5.79 ng/L, $p = 0.6377$), T3S1A (surface vs bottom; 3.99 ng/L vs 5.17 ng/L, $p = 0.2402$) and T1S2A (surface vs bottom; 3.27 ng/L vs 4.20 ng/L, $p = 0.2402$) in offshore areas doesn't follow the surface enrichment model proposed, likely because they're close to recreational areas (e.g., swimming) characterized by water disturbance and particulate resuspension. In general, 25 out of 35 stations sampled in the Biscayne Bay and offshore showed a depth

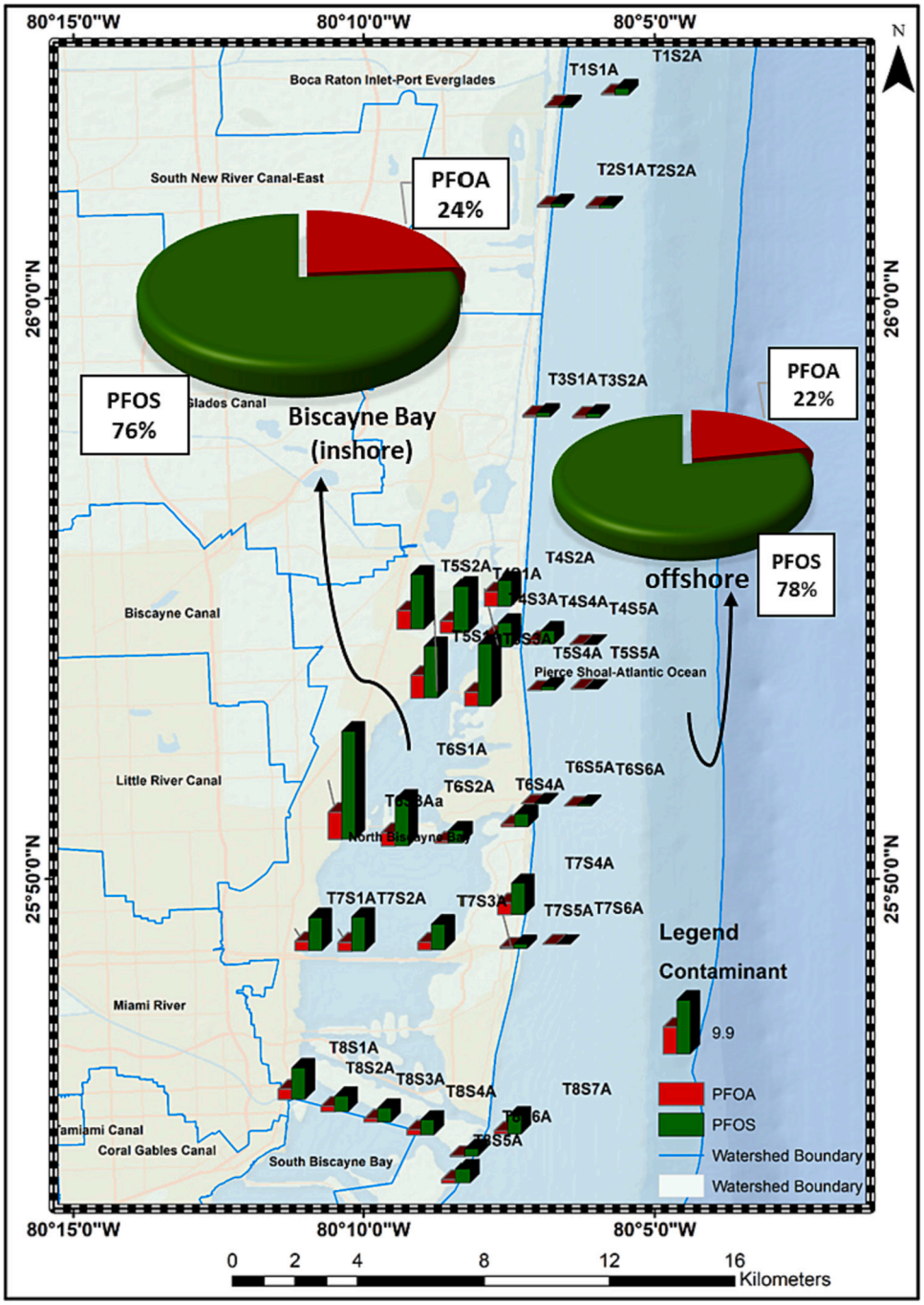

Fig. 7. Spatial distribution and transport of Legacy PFOS and PFOA (linear+ branched) profile in surface water from inshore to coastal environment.

depletion patterns (~71 %) except for 10 stations-T8S6, T8S5, T8S4, T8S3, T7S4, T7S2, T6S4 and T6S3, T3S1 and T1S2.

3.3. Spatial distribution, occurrence, and transport of legacy PFOS and PFOA in surface water

The spatial distribution of PFOA and PFOS (branched + linear) is shown in Fig. 7. From all the 30 PFAS analyzed, ∑PFOS had the highest mean concentration both inshore (6.36 ± 4.22 ng/L) and offshore (0.83 ± 0.87 ng/L) with detection frequency of 100 % and 87.5 % inshore and offshore, respectively. As previously stated, ∑PFAS was highest at station T6S1A. PFOS was the most prevalent of all the measured PFAS in this site compared to other locations- inshore and offshore. It can also be noted that stations in the northward section (inshore) also displayed high values of PFOS and PFOA after station T6S1A. These stations include T5S1A, T5S2A, T5S3A, T4S1A, T4S2A and T4S3A located at the opening of Biscayne canal and Arch creek. The freshwater input from Miami river, Little river, and Snake creek (52.6 % of total freshwater intrusion into the Biscayne Bay) is basically characterized with urban stormwater runoffs, land fill leachates and sewage contamination (Caccia and Boyer, 2007). This explains the high levels of legacy PFOA and PFOS observed close to the shoreline of these canals. The concentration of PFOA and PFOS dilutes from west to east (coastal areas) in all the transects highlighted in the map except for station Ta5S3A (11.39 ng/L), T6S4A (2.32 ng/L) and T7S4A (5.75 ng/L), which are strategically located among urbanized settlements, solid waste facilities and Miami beach area. The water samples collected in these regions were characterized by high turbidity, blue-greenish algae coloration suggesting the influence of anthropogenic discharge from highly urbanized settlements and solid waste leachates contributing to a greater extent, to an increase in the levels of legacy PFAS loadings. PFOA and PFOS were initially used as active chemicals in personal care products, surface protection products such as cookware, clothing, carpet, and food packaging materials (Pennsylvania Department of Health, 2023). PFOS was majorly used in electronics cleaning and petrochemical and textile treatment industry (Liu et al., 2017). High levels of PFOS have been reported in coastal environments (Liu et al., 2022). Although both PFOA and PFOS are soluble in surface water with longer resident time, our results indicate that PFOS>PFOA, suggesting that PFOS-contained materials are still in active use in domestic and industrial products consumed in the surrounding areas. Furthermore, PFOS/PFOA ratio has been previously adopted in published literature to access point source of PFOS pollution (Liu et al., 2022; Yang et al., 2020). The ratio PFOS/PFOA >1 indicates point source pollution while PFOS/PFOA <1 indicates PFOS contamination through rainfall. The values obtained for PFOS/PFOA ratio inshore (3.22) and offshore (3.57) suggest that rainfall had little contribution to PFOS loadings observed in our study area. Hence, anthropogenic inputs because of heavy urbanization, landfill leachates and sewage discharge from domestic wastewater (especially prominent in Miami river) and wastewater treatment plants (WWTPs) are likely the major point source of PFOS contamination. Mann-Whitney two-tailed test ($\alpha = 0.05$) indicates statistical difference ($p < 0.05$) between the average ∑PFOS (inshore vs offshore; 6.36 ± 4.22 ng/L vs 0.83 ± 0.87 ng/L) and average ∑PFOA (inshore vs offshore; 1.97 ± 1.23 ng/L vs 0.23 ± 0.18 ng/L). As shown in Fig. 7, PFOS contributes 76 % while PFOA contributes 24 % to ∑ legacy PFAS burden inshore while offshore PFOS and PFOA contributes 78 % and 22 %, respectively.

3.4. Clustering analysis and source identification of PFAS in inshore and offshore area of Biscayne Bay

Cluster analysis is a typical form of data reduction techniques used to distinctively identify homogeneous or similar subgroups in a given population. In other words, datasets with similar attributes are grouped together and it often provides a great starting point for exploratory and statistical analysis. In our study we used k-means clustering to assess similarities between stations sampled inshore and offshore in terms of PFAS fingerprints; each cluster has similar compositional profiles that are distinct from other clusters. PFAS found predominant in each cluster can then be used as tracers of potential point sources of discharges into the Biscayne Bay. Increase in the number of clusters decreases the variational difference within the cluster (Gibson et al., 2019). To minimize variation within cluster, we chose four clusters (k = 4) for the analysis of inshore samples while three clusters (k = 3) were used for offshore samples as shown in Figs. 8 and 9, respectively.

Since the canals are the entry point of PFAS discharge into the Biscayne Bay, it was interesting to observe difference in PFAS fingerprints at the stations close to these canals. According to the Florida Department of Environmental Protection (FDEP), these canals were ascribed a unique waterbody identification (WBID) number (Table S9) and named as: C-6 (Miami) canal, C-7 (Little River) canal, C-8 (Biscayne) canal, and C-9 (Snake Creek) canal. From our observations, station T6S1A (C-7) and T5S1A (C-8) have similar PFAS composition; same as T8S1A (C-6), T7S1A and T4S1A (Arch creek/C-9). Although T6S1A and T5S1A are located at the mouth of two different canals (C-7 and C-8 respectively), they cluster together suggesting common potential source of PFAS contamination and discharge into the Bay. Sewage contamination (through failed septic systems) from urbanized settlements were previously reported as point source of freshwater drain into these two canals (Caccia and Boyer, 2007; Wachnicka et al., 2020). Furthermore, according to the FDEP's land development intensity index (LDI) of 5.2–6.9, these areas (Fig. S4) are characterized by row crops (agricultural), low density residential and high intensity recreational activities, thus, suggesting the impact and source contribution of unique PFAS fingerprints to the C-7 and C-8 canals respectively. This cluster (cluster 1) had the highest concentration of the following compounds (Fig. S5): PFOS, PFOA, PFPeA, PFHxS, PFHxA, PFBA and PFBS which are actively used as stain and grease repellants, surfactants, carpets, food packaging and household products (U.S.EPA, 2021). Cluster 2 is mostly representative of bottom water samples. It should be noted that cluster 3 and 4 had the highest concentration of FOSA (3.75 and 6.25 ng/L respectively) as a distinct compound from other clusters. FOSA is primarily used as water and grease repellants in food packaging materials and a precursor of PFOS (Xu et al., 2006). This suggests that food packaging materials from household and commercial use are potential sources of PFAS contamination in Biscayne Bay. Additionally, T8S1A, T7S1A (located at the mouth of C-6) and T4S1A (at the intersect of Arch creek and C- 9) have similar PFAS fingerprints (cluster 3). The similarity in PFAS composition observed in these canals might be associated with their connection to similar drainage channels spanning from the Everglades National Park and conservation area. Furthermore, the LDI of 7.8–8.7 (Fig. S5) suggests the influence of residential, industrial, and institutional influence as source contribution of PFAS patterns seen in these canals. It's also interesting to note that cluster 3 had the highest concentration of 6–2 FTS (4.38 ng/L) which is one of the major constituents currently used in aqueous film forming foam (AFFF) in military and airport facilities. This suggests that surface run-off from Miami international airport which drains into the C-6 canal could be a potential source of PFAS contamination into the Bay. Regarding offshore clusters (Fig. S6), FOSA was present in cluster 1 (extension of transect 8) and cluster 2 also suggesting contamination from food packaging materials; FOSA could also metabolize to contribute to the levels of PFOS observed offshore especially among cluster 1 stations. Although ∑C9-C14 PFAS appears to be the highest in all the clusters offshore, PFOS was highest in terms of the individual PFAS analyzed. One-way ANOVA (Kruskal Wallis) test was used for testing statistical difference of individual PFAS between the clusters (Table S10); there was statistical significance for all compounds inshore ($p < 0.05$) except for FOSA. Similarly, all PFAS from offshore clusters are statistically significant ($p < 0.05$) except for C9-C14 compounds. The Tukey HSD post-hoc analysis was also conducted to show which cluster pair was influencing the significant difference observed for each individual PFAS inshore and offshore (Fig. S7 and S8). This

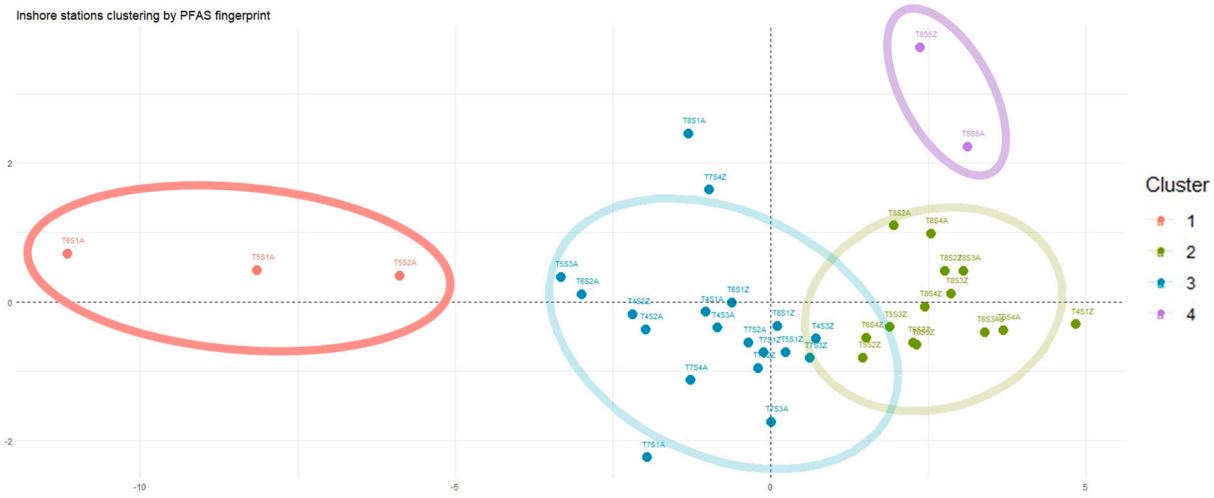

Fig. 8. K-Means clustering showing stations in the Biscayne Bay with similar PFAS fingerprints grouped into five clusters.

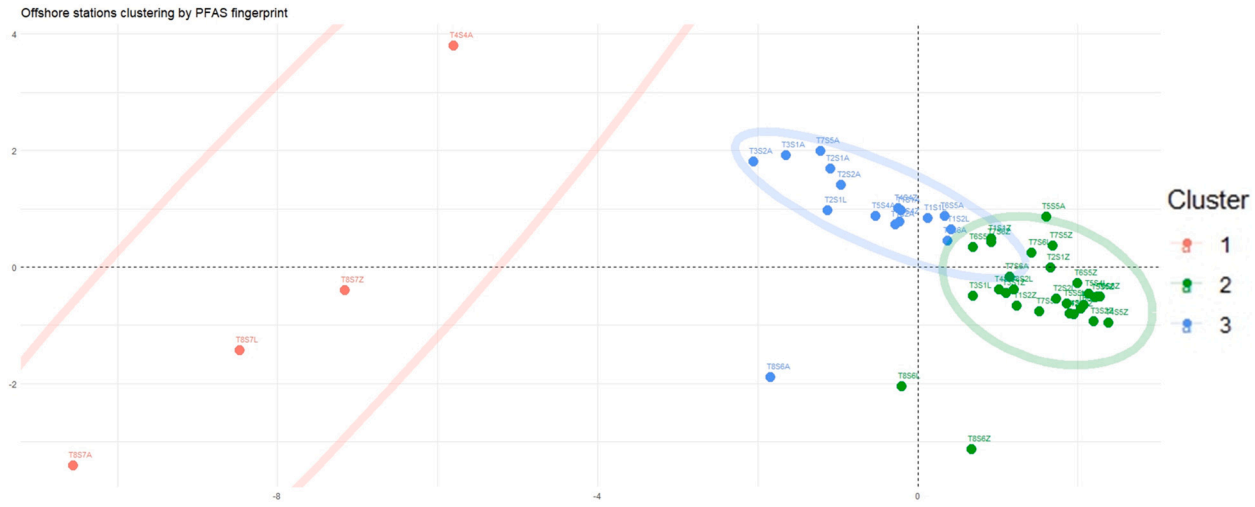

Fig. 9. K-Means clustering showing stations in offshore areas of Biscayne Bay with similar PFAS fingerprints grouped into three clusters.

implies that cluster pairs that didn't cross the 0-axis vertical line contribute the most significance to the levels of each PFAS observed.

3.5. Trends of thermohaline parameters from inshore Biscayne Bay to offshore areas and correlations on PFAS occurrence and dispersion with salinity

Temperature and salinity are important parameters for measuring water quality, especially in coastal environments. While temperature measures heat exchange, salinity provides insights on dilution and movement of waters in the coastal area (Woody et al., 2000) (Woody et al., 2000). Hence, they can serve as potential indicators of mixing, transport, and stratification of water bodies. In our study, salinity and temperature parameters were measured inshore and offshore Biscayne Bay area during the wet season (summer), which spans from May to October in Florida. The northern part of the Biscayne Bay is influenced by freshwater inputs from the Creeks (Snake and Arch), Biscayne canal, Little River, and Miami River. Therefore, areas that are near the canals exhibit low salinity and high-salinity fluctuations (Fig. S9A-E). Gradual increase in salinity was observed at all transects as we migrate from nearshore (left) to offshore (right) areas due to influx of oceanic waters from the Atlantic Ocean which are characterized by less variability in salinity and high-mean salinity (Lirman et al., 2008). Vertical profile of salinity suggests a gradual increase in salinity with depth due to replacement of freshwater by inflow of dense-salty water from the oceanic water entering the bay as observed in all the transects in our study area. There is also possibility of mixing since the Bay is quite shallow due to the influence of wind, waves, and ocean current. Salinity levels increased in Transect 8 compared to other areas since there's direct exchange with the Atlantic Ocean through the valves. Unlike salinity, temperature declined gradually within the bay to offshore in all transects both horizontally and vertically (Fig. S10F-J. Although there was a gradual drop, no thermocline was observed suggesting that the water column is fairly mixed. Also, fluctuations were also observed at different stations within the bay (30-31 °C) due to the influence of wind and ocean current while offshore (28-29 °C) showed a lower temperature profile due to interaction of the water column with strong tidal waves and wind.

To understand the relationship between individual PFAS, ∑PFAS and salinity, Spearman rank correlation plot was applied (Fig. 10). This is depicted using $-1 < \rho < +1$. Where a ρ value of +1 indicates that there is a perfect positive association between ranks, $\rho = 0$ indicates no association of ranks and a $\rho = +1$ indicates a perfect negative association. The closer the ρ to 0, the weaker is the association between two ranks. Applying the Quinnipiac University ranks for ρ, our findings (Fig. 10) shows that PFOS, PFBA, PFPeA, PFHxA, ∑PFAS, PFOA, PFBS, PFHxS

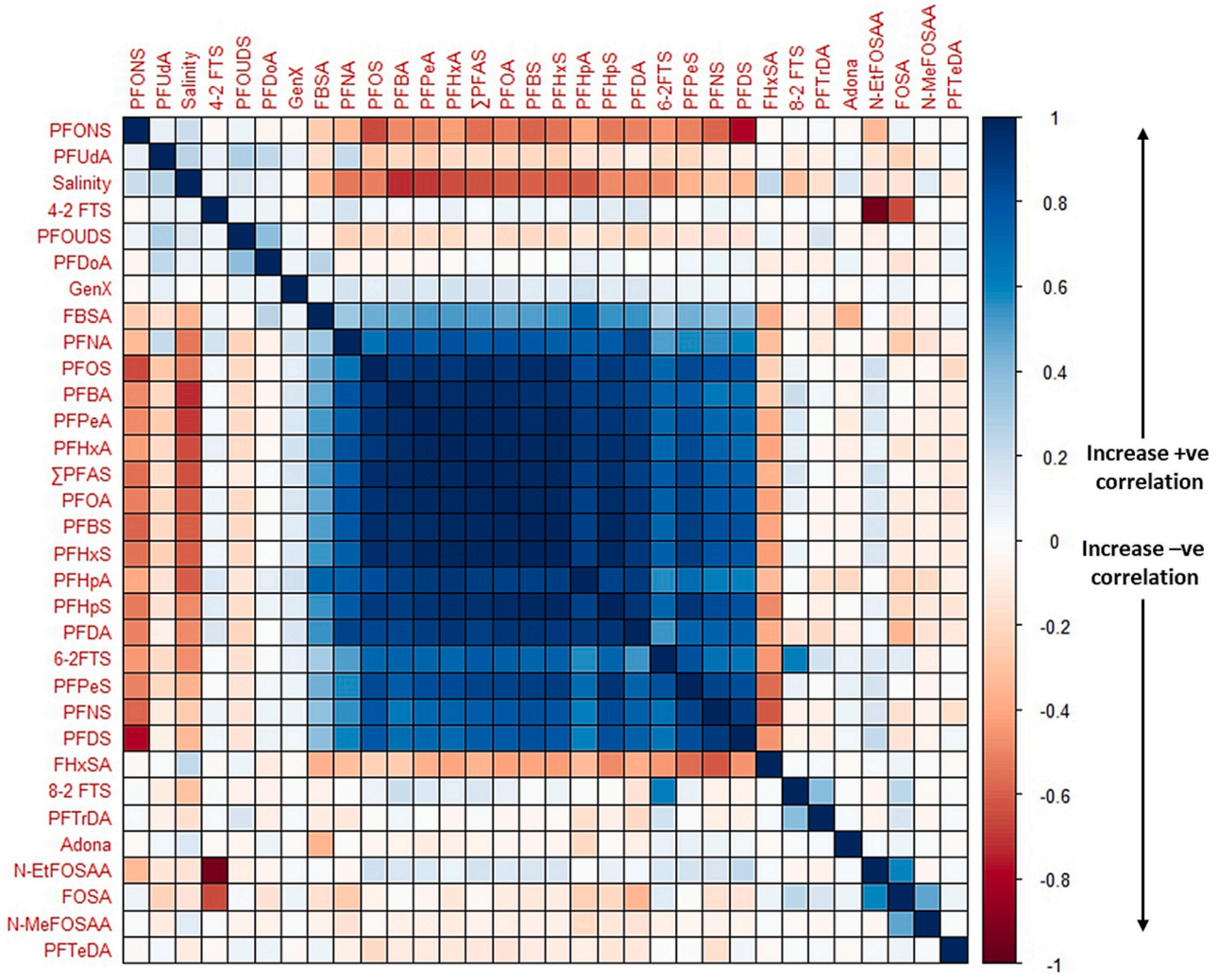

Fig. 10. Spearman Rank Correlation plot showing the relationship between individual PFAS, ∑PFAS loadings and salinity.

and PFHpS all show a very strong positive correlation among each other ($\rho > 0.7$), suggesting that they have similar chemistry and sources. Comparing the relationship of PFAS with salinity, PFBA, PFPeA, PFHxA, ∑PFAS, PFOA, PFBS, PFHxS and PFHpA showed a strong negative correlation with salinity ($\rho = -0.6$ to -0.5), and PFOS, PFNA, PFHpS, PFDA and 6–2 FTS, have moderate negative correlation ($\rho = -0.3$), while PFPeS, FBSA, PFNS and PFDS ($\rho = -0.2$ to -0.1) showed weak correlations. According to Yin et al., increase in salinity can neutralize negatively charged surfaces on sediments, which enhances the adsorption of anionic PFAS due to reduction of electrostatic repulsion on sorbent-PFAS interface (Yin et al., 2022). This implies that increased salinity can increase PFAS-sediment sorption and reduce their concentration in water. This explains the inverse (negative) correlation of salinity with some PFAS observed in our study. It is expected that lower PFAS concentration should be observed in bottom profiles due to higher salinity content, however other factors such as downward migration of particulate matter, wind action and eddy diffusion could play stronger influence. Furthermore, increased salinity could decrease the solubility of PFAS through electrostatic interactions with water molecules.

3.6. Forecasting PFAS dispersion across source points (inshore) to offshore Biscayne Bay area based on ocean currents

As stated, we observed the highest ∑PFAS loadings from point sources such as the artificial and natural canals westward of the Biscayne Bay, and lowest ∑PFAS loadings in offshore, coastal environments. Here, we have then applied an Inverse distance weighted interpolation (IDW) to model and forecast the general dispersion and distribution of ∑PFAS loadings in our study area (25^0 N–26^0 N and 80^0 N–85^0 N). The IDW approach explicitly assumes that things that are near each other are more likely similar than those that are further apart. As shown in Fig. 11A and Fig. 11B, our result indicates that the highest ∑PFAS discharge into the northern section of the Biscayne Bay comes from the Little river canal followed by the Biscayne canal and the Miami river and dilutes eastward towards the Atlantic ocean. Although the major tidal exchange between Biscayne Bay and the Atlantic Ocean usually occurs at the safety valves (located in the central section of the Biscayne Bay), significant tidal exchange can also occur at the opening along the government cut (close to Miami port), the Rickenbacker axis (the valve directly above the safety valve) and the Haulover opening (up-North) as indicated by our forecast. This can ultimately lead to the transport of PFAS from inshore to offshore. It is also interesting to conclude that point sources are the major contribution to ∑PFAS (including legacy and emerging compounds) pollution burden in the Biscayne Bay and coastal areas.

4. Comparison of coastal concentrations of PFAS

The temporal trends of PFAS are important in understanding the fate and transport of these contaminants in coastal environment as well as

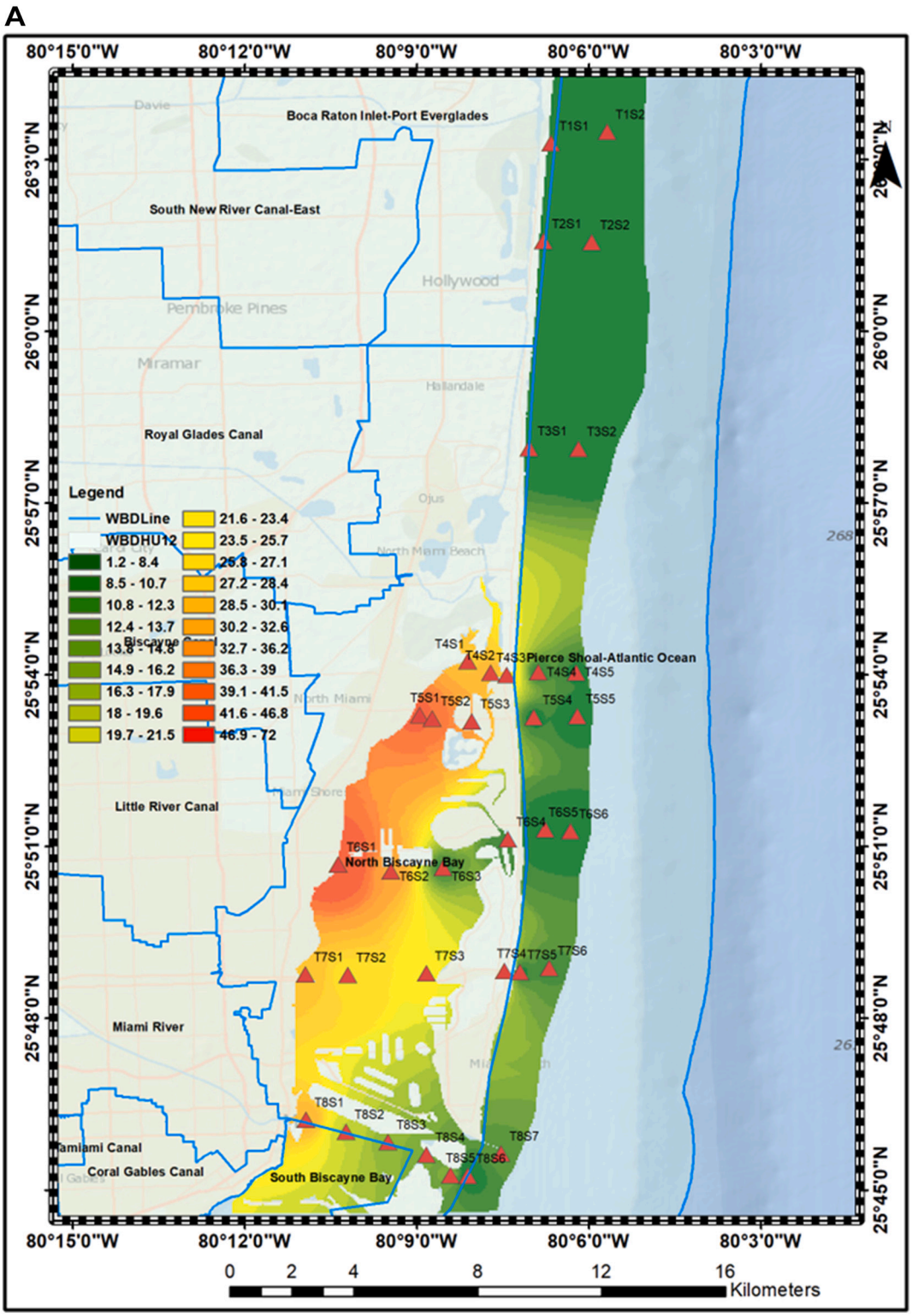

Fig. 11A. Surface profile showing the dispersion and distribution of ∑PFAS forecast from point sources, inshore to offshore Biscayne Bay.

assessing whether effective management efforts are being enacted to reduce and eliminate the manufacture, use and discharge of PFAS in the environment. Research conducted in coastal and open marine environments around the world is very limited but has reported significant concentration of PFAS in surface water samples. Muir et al. posited that PFOS, PFOA and FOSA constitute about 83 % of all measured PFAS in coastal water (Muir and Miaz, 2021). Although there are limited information on PFSAs and PFCAs in coastal South and North America, high mean concentrations of ∑PFSAs (~9.5 ng/L) and ∑C7-C12 PFCAs (~10.2 ng/L) in year 2010–2014 were reported in Yellow and Bohai Seas; recent repeated studies from 2015 to 2019 indicates same trends for ∑PFSAs (~1.2 ng/L) and ∑C7-C12 PFCAs (~10.5 ng/L) compared to other coastal waters reported by Muir and Miaz (2021). Elevated concentration was due to the presence of PFPeA, PFBA and PFOA. High mean levels of PFOS and ∑PFSAs (~3–6 ng/L) were also reported in Western Europe especially in coastal waters and estuary influenced by

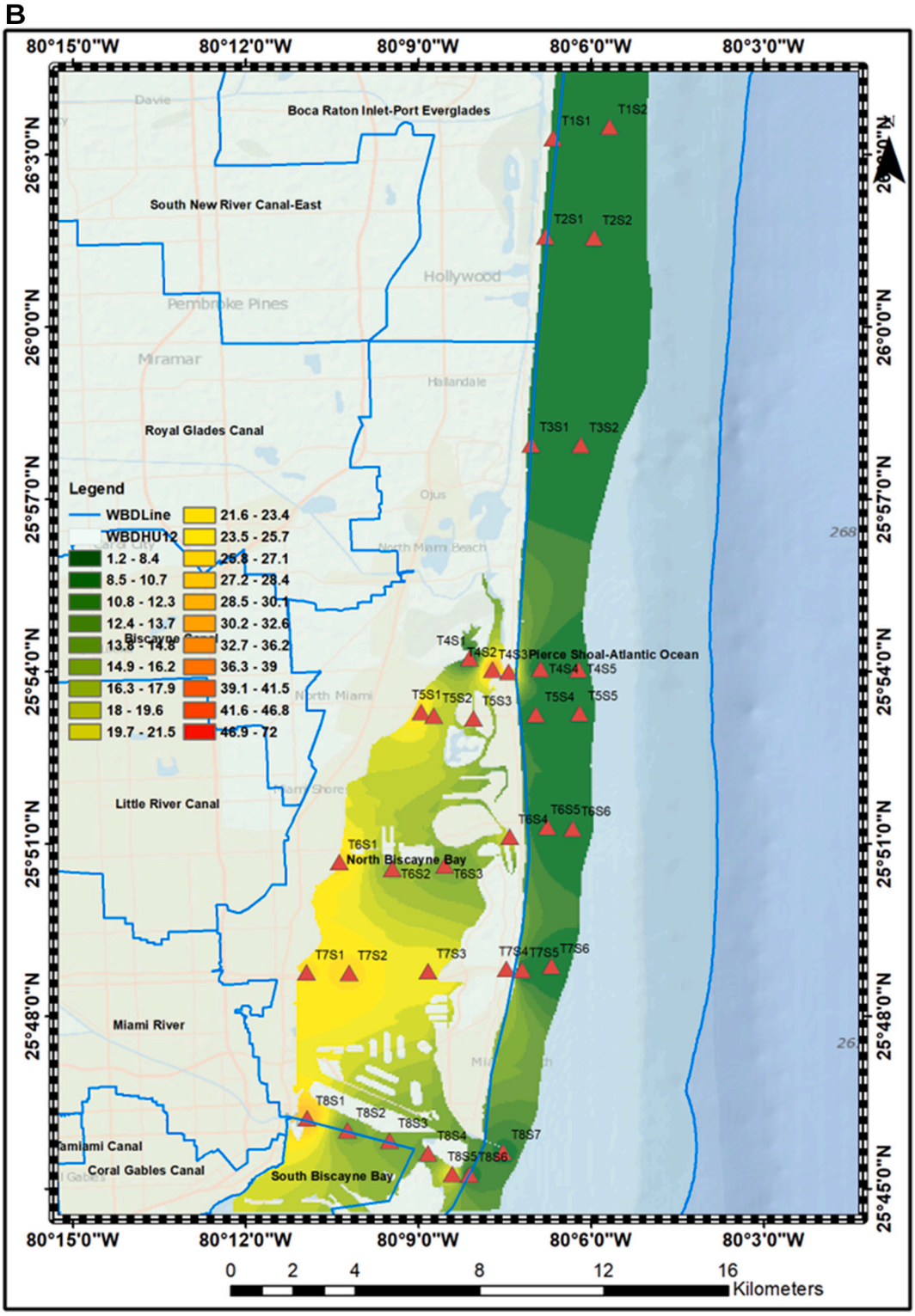

Fig. 11B. Bottom profile showing the dispersion and distribution of ∑PFAS forecast from point sources, inshore to offshore Biscayne Bay.

heavy urbanization (Muir and Miaz, 2021). Comparing these results with our study in coastal Biscayne Bay, we have observed that the levels of ∑PFSAs (2.05 ng/L) and ∑PFCAs (3.12 ng/L) are lower than that of Western Europe. Furthermore, the ∑PFAS reported in Biscayne Bay (29.52 ng/L) and coastal areas (5.17 ng/L) were lower than those reported in coastal areas of China and South Korea (14.9 to 16,500 ng/L) (Shi et al., 2021). Although the levels reported in our location are lower compared to few other coastal environments, an informed action plan needs to be implemented to minimize these levels before they begin to cause ecological and human impact.

5. Conclusion

In summary, we investigated the occurrence, dispersion, vertical distribution and identified point sources of PFAS discharge by conducting a spatial transect from West to East of Biscayne Bay, Miami

Dade, in Florida, U.S. Average ∑PFAS loadings inshore (surface vs bottom; 29.52 ± 15.25 ng/L vs 21.45 ± 7.85 ng/L) was significantly higher than offshore (surface vs bottom; 5.17 ± 2.66 ng/L vs 2.20 ± 1.60 ng/L). The high PFAS burden in Biscayne Bay is due to direct discharge of freshwater from adjacent canals which dilutes Eastward towards the Atlantic Ocean. PFOS had the highest concentration both inshore (19.84 ng/L) and offshore (3.30 ng/L). The most frequently detected (D·F > 94 %) PFAS were PFBA, PFPeA, PFHxA, PFHpA, PFOA, PFNA, PFBS, PFHxS, and PFOS in surface water samples. In general, a vertical, downward decline in PFAS concentration was observed for surface and bottom water samples. k-means clustering analysis suggests distinct PFAS compositional profile among clusters and especially at the canals reported in this study. We further corroborated this finding using the FDEP's LDI for source contamination of PFAS. Tracers recommended as potential candidates for identifying point sources of discharge of PFAS into Biscayne Bay through the canals includes: PFCAs (PFBA, PFPeA, PFHxA, PFHpA, PFOA, and PFNA) and PFSAs (PFBS, PFHxS, and PFOS). This can be of tremendous help in tracking PFAS patterns to point sources identified in our research and along constructional tributaries and channels leading into the Bay. Potential point sources of discharge into Biscayne Bay are from domestic wastewater, WWTPs, failing septic systems, airports, and military facilities. Furthermore, PFOS/PFOA also confirms that the major contribution to PFAS burden in Biscayne Bay are from point sources although, we also acknowledge that precipitation can play a role in PFAS loadings. From human health and ecological perspective, the mean levels of PFOS (6.36 ± 4.23 ng/L) and PFOA (1.97 ± 1.23 ng/L) inshore reported in this study is below the Florida Department of Environmental Protection (FDEP) advisory levels in surface water for Human health exposure (PFOS: 10 ng/L and PFOA: 500 ng/L) and freshwater (PFOS: 3.7×10^4 ng/L and PFOA: 1.3×10^6 ng/L), however these levels might not be protective of human and marine life and informed action plan should be implemented to prevent deleterious effects to both human and aquatic life in Biscayne Bay.

Supplementary data to this article can be found online at https://doi.org/10.1016/j.scitotenv.2023.168413.

Declaration of competing interest

The authors declare that they have no known competing financial interests or personal relationships that could have appeared to influence the work reported in this paper.

Data availability

Data will be made available on request.

Acknowledgements

We would like to acknowledge the financial support of FIU CREST Center for Aquatic Chemistry and the Institute of Environment for providing us with fieldwork grant to collect samples at Biscayne Bay. Special appreciation goes to William Chamberlain, Annie Sevon, and the entire crew team- Leila, Maria and Neumiah for their numerous supports during the sampling campaign. This material is based upon work supported by the National Science Foundation under Grant No. HRD-1547798 and Grant No. HRD-2111661. These NSF Grants were awarded to Florida International University as part of the Centers of Research Excellence in Science and Technology (CREST) Program. This is contribution number #1663 from the Institute of Environment at Florida International University.

Credit author statement

Olutobi Daniel Ogunbiyi: Investigation, Methodology, Validation, Data Curation, Visualization, Formal analysis, Writing - Original Draft, Writing – Draft reviewing; **Neumiah Massenat:** Investigation, Methodology, Formal analysis, Review; **Natalia Quinete:** Conceptualization, Methodology, Validation, Data Curation, Project administration, Supervision, Resources, Writing – Original Draft Review & Editing.

References

Caccia, V.G., Boyer, J.N., 2005. Spatial patterning of water quality in Biscayne Bay, Florida as a function of land use and water management. Mar. Pollut. Bull. 50, 1416–1429. https://doi.org/10.1016/j.marpolbul.2005.08.002.

Caccia, V.G., Boyer, J.N., 2007. A nutrient loading budget for Biscayne Bay, Florida. Mar. Pollut. Bull. 54, 994–1008. https://doi.org/10.1016/j.marpolbul.2007.02.009.

Chang, E.T., Adami, H.O., Boffetta, P., Wedner, H.J., Mandel, J.S., 2016. A critical review of perfluorooctanoate and perfluorooctanesulfonate exposure and immunological health conditions in humans. Crit. Rev. Toxicol. https://doi.org/10.3109/10408444.2015.1122573.

Chiumiento, F., Bellocci, M., Ceci, R., D'Antonio, S., De Benedictis, A., Leva, M., Pirito, L., Rosato, R., Scarpone, R., Scortichini, G., Tammaro, G., Diletti, G., 2023. A new method for determining PFASs by UHPLC-HRMS (Q-Orbitrap): application to PFAS analysis of organic and conventional eggs sold in Italy. Food Chem. 401 https://doi.org/10.1016/j.foodchem.2022.134135.

Gibson, E.A., Nunez, Y., Abuawad, A., Zota, A.R., Renzetti, S., Devick, K.L., Gennings, C., Goldsmith, J., Coull, B.A., Kioumourtzoglou, M.A., 2019. An overview of methods to address distinct research questions on environmental mixtures: an application to persistent organic pollutants and leukocyte telomere length. Environ. Health. https://doi.org/10.1186/s12940-019-0515-1.

Göckener, B., Fliedner, A., Rüdel, H., Badry, A., Koschorreck, J., 2022. Long-term trends of per- and Polyfluoroalkyl substances (PFAS) in suspended particular matter from German Rivers using the direct Total Oxidizable precursor (dTOP) assay. Environ. Sci. Technol. 56, 208–217. https://doi.org/10.1021/acs.est.1c04165.

Han, T., Chen, J., Lin, K., He, X., Li, S., Xu, T., Xin, M., Wang, B., Liu, C., Wang, J., 2022. Spatial distribution, vertical profiles and transport of legacy and emerging per- and polyfluoroalkyl substances in the Indian Ocean. J. Hazard. Mater. 437, 129264 https://doi.org/10.1016/j.jhazmat.2022.129264.

Herzke, D., Nikiforov, V., Yeung, L.W.Y., Moe, B., Routti, H., Nygård, T., Gabrielsen Geir, W., Hanssen, L., 2023. Targeted PFAS analyses and extractable organofluorine – enhancing our understanding of the presence of unknown PFAS in Norwegian wildlife. Environ. Int. 171, 107640 https://doi.org/10.1016/j.envint.2022.107640.

Joerss, H., Xie, Z., Wagner, C.C., Von Appen, W., Sunderland, E.M., Ebinghaus, R., 2020. Transport of Legacy per Fluoroalkyl Substances and the Replacement Compound HFPO-DA through the Atlantic Gateway to the Arctic Ocean: Is the Arctic a Sink or a Source? https://doi.org/10.1021/acs.est.0c00228.

Lenka, S.P., Kah, M., Padhye, L.P., 2021. A review of the occurrence, transformation, and removal of poly- and perfluoroalkyl substances (PFAS) in wastewater treatment plants. Water Res. https://doi.org/10.1016/j.watres.2021.117187.

Lescord, G.L., Kidd, K.A., De Silva, A.O., Williamson, M., Spencer, C., Wang, X., Muir, D. C.G., 2015. Perfluorinated and polyfluorinated compounds in lake food webs from the Canadian high Arctic. Environ. Sci. Technol. 49, 2694–2702. https://doi.org/10.1021/es5048649.

Li, F., Duan, J., Tian, S., Ji, H., Zhu, Y., Wei, Z., Zhao, D., 2020. Short-chain per- and polyfluoroalkyl substances in aquatic systems: occurrence, impacts and treatment. Chem. Eng. J. https://doi.org/10.1016/j.cej.2019.122506.

Li, X., Fatowe, M., Cui, D., Quinete, N., 2022. Assessment of per- and polyfluoroalkyl substances in Biscayne Bay surface waters and tap waters from South Florida. Sci. Total Environ. 806, 150393 https://doi.org/10.1016/j.scitotenv.2021.150393.

Lirman, D., Deangelo, G., Serafy, J., Hazra, A., Smith Hazra, D., Herlan, J., Luo, J., Bellmund, S., Wang, J., Clausing, R., 2008. Seasonal changes in the abundance and distribution of submerged aquatic vegetation in a highly managed coastal lagoon. Hydrobiologia 596, 105–120. https://doi.org/10.1007/s10750-007-9061-x.

Liu, Z., Lu, Y., Wang, P., Wang, T., Liu, S., Johnson, A.C., Sweetman, A.J., Baninla, Y., 2017. Pollution pathways and release estimation of perfluorooctane sulfonate (PFOS) and perfluorooctanoic acid (PFOA) in central and eastern China. Sci. Total Environ. 580, 1247–1256. https://doi.org/10.1016/j.scitotenv.2016.12.085.

Liu, Z., Zhou, J., Xu, Y., Lu, J., Chen, J., Wang, J., 2022. Distributions and sources of traditional and emerging per- and polyfluoroalkyl substances among multiple environmental media in the Qiantang River watershed, China. RSC Adv. 12, 21247–21254. https://doi.org/10.1039/d2ra02385g.

Lorenzo, M., Campo, J., Morales Suárez-Varela, M., Picó, Y., 2019. Occurrence, distribution and behavior of emerging persistent organic pollutants (POPs) in a Mediterranean wetland protected area. Sci. Total Environ. 646, 1009–1020. https://doi.org/10.1016/j.scitotenv.2018.07.304.

Louisse, J., Rijkers, D., Stoopen, G., Janssen, A., Staats, M., Hoogenboom, R., Kersten, S., Peijnenburg, A., 2020. Perfluorooctanoic acid (PFOA), perfluorooctane sulfonic acid (PFOS), and perfluorononanoic acid (PFNA) increase triglyceride levels and decrease cholesterogenic gene expression in human HepaRG liver cells. Arch. Toxicol. 94, 3137–3155. https://doi.org/10.1007/s00204-020-02808-0.

Mcpherson, B.F., Hendrix, G.Y., Klein, H., Tyus, H.M., 1976. The Environment of South Florida, As Ry Epo T.

Muir, D., Miaz, L.T., 2021. Spatial and temporal trends of Perfluoroalkyl substances in Global Ocean and coastal waters. Environ. Sci. Technol. 55, 9527–9537. https://doi.org/10.1021/acs.est.0c08035.

Ng, B., Quinete, N., Gardinali, P., 2022. Differential organic contaminant ionization source detection and identification in environmental waters by nontargeted analysis. Environ. Toxicol. Chem. 41, 1154–1164. https://doi.org/10.1002/etc.5268.

NOAA (2023). National Data Buoy Center. https://www.ndbc.noaa.gov/view_text_file.php?filename=vakf1h2022.txt.gz&dir=data/historical/stdmet/ (accessed 10.20.23).

Ogunbiyi, O.D., Ajiboye, T.O., Omotola, E.O., Oladoye, P.O., Olanrewaju, C.A., Quinete, N., 2023. Analytical approaches for screening of per- and poly fluoroalkyl substances in food items: a review of recent advances and improvements. Environ. Pollut. https://doi.org/10.1016/j.envpol.2023.121705.

Pennsylvania Department of Health, 2023. PFAS Fact Sheet. Pennsylvania Department of Health, pp. 1–9.

Rundle, K.F., Horn, D.L., Rosen, H., Maer, D., Perikles, J., 2019. THE HEALTH OF BISCAYNE BAY: WATER FLOWS AND WATER WOES, pp. 1–27.

Savvidou, E.K., Sha, B., Salter, M.E., Cousins, I.T., Johansson, J.H., 2023. Horizontal and vertical distribution of Perfluoroalkyl acids (PFAAs) in the water column of the Atlantic Ocean. Environ. Sci. Technol. Lett. 10, 418–424. https://doi.org/10.1021/acs.estlett.3c00119.

Scher, D.P., Kelly, J.E., Huset, C.A., Barry, K.M., Hoffbeck, R.W., Yingling, V.L., Messing, R.B., 2018. Occurrence of perfluoroalkyl substances (PFAS) in garden produce at homes with a history of PFAS-contaminated drinking water. Chemosphere 196, 548–555. https://doi.org/10.1016/j.chemosphere.2017.12.179.

Shi, B., Wang, T., Yang, H., Zhou, Y., Bi, R., Yang, L., Yoon, S.J., Kim, T., Khim, J.S., 2021. Perfluoroalkyl acids in rapidly developing coastal areas of China and South Korea: spatiotemporal variation and source apportionment. Sci. Total Environ. 761 https://doi.org/10.1016/j.scitotenv.2020.143297.

Susmann, H.P., Schaider, L.A., Rodgers, K.M., Rudel, R.A., 2019. Dietary habits related to food packaging and population exposure to PFASs. Environ. Health Perspect. 127 https://doi.org/10.1289/EHP4092.

U.S.EPA,, 2021. Systematic review protocol for the for the PFAS IRIS Assessments. U.S. Environmental Protection Agency, Washington, DC, EPA/635/R-19/050, 2019.

Wachnicka, A., Browder, J., Jackson, T., Louda, W., Kelble, C., Abdelrahman, O., Stabenau, E., Avila, C., 2020. Hurricane Irma's impact on water quality and phytoplankton communities in Biscayne Bay (Florida, USA). Estuar. Coasts 43, 1217–1234. https://doi.org/10.1007/s12237-019-00592-4.

Woody, C., Shih, E., Miller, J., Royer, T., Atkinson, L.P., Moody, R.S., 2000. Measurements of salinity in the Coastal Ocean: a review of measurements of salinity in the Coastal Ocean: a review of requirements and technologies requirements and technologies part of the fresh water studies commons, and the oceanography commons original publication citation original publication citation measurements of salinity in the coastal ocean: a review of requirements and technologies. Mar. Technol. Soc. 34 (2), 26–33.

Xu, L., Krenitsky, D.M., Seacat, A.M., Butenhoff, J.L., Tephly, T.R., Anders, M.W., 2006. N-glucuronidation of perfluorooctanesulfonamide by human, rat, dog, and monkey liver microsomes and by expressed rat and human UDP- glucuronosyltransferases. Drug Metab. Dispos. 34, 1406–1410. https://doi.org/10.1124/dmd.106.009399.

Yamazaki, E., Taniyasu, S., Ruan, Y., Wang, Q., Petrick, G., Tanhua, T., Gamo, T., Wang, X., Lam, P.K.S., Yamashita, N., 2019. Vertical distribution of perfluoroalkyl substances in water columns around the Japan Sea and the Mediterranean Sea. Chemosphere 231, 487–494. https://doi.org/10.1016/j.chemosphere.2019.05.132.

Yang, Q.Q., Wang, S.L., Liu, W.J., Yang, Y.W., Jiang, S.Q., 2020. Spatial distribution of perfluoroalkyl acids (PFAAs) and their precursors and conversion of precursors in seawater deeply affected by a city in China. Ecotoxicol. Environ. Saf. 194 https://doi.org/10.1016/j.ecoenv.2020.110404.

Yin, C., Pan, C.G., Xiao, S.K., Wu, Q., Tan, H.M., Yu, K., 2022. Insights into the effects of salinity on the sorption and desorption of legacy and emerging per-and polyfluoroalkyl substances (PFASs) on marine sediments. Environ. Pollut. 300, 118957 https://doi.org/10.1016/J.ENVPOL.2022.118957.

Zhang, X., Lohmann, R., Sunderland, E.M., 2019. Poly- and Perfluoroalkyl substances in seawater and plankton from the northwestern Atlantic margin. Environ. Sci. Technol. 53, 12348–12356. https://doi.org/10.1021/acs.est.9b03230.

Zhao, Z., Xie, Z., Möller, A., Sturm, R., Tang, J., Zhang, G., Ebinghaus, R., 2012. Distribution and long-range transport of poly fl uoroalkyl substances in the Arctic. Atlantic Ocean and Antarctic Coast 170, 71–77. https://doi.org/10.1016/j.envpol.2012.06.004.